

Classification of some Iranian *Vicia* species using SEM image analysis coupled with conventional texture analysis and deep learning

Mehrnoosh Jafari^{1*}, Seyed Ali Mohammad Mirmohammady Maibody², and Mohammad Hossein Ehtemam²

1. Department of Biosystems Engineering, College of Agriculture, Isfahan University of Technology, Isfahan 84156-83111, Islamic Republic of Iran.

*Corresponding Author; e-mail: m.jafari@iut.ac.ir

2. Department of Agronomy and Plant Breeding, College of Agriculture, Isfahan University of Technology, Isfahan 84156-83111, Islamic Republic of Iran.

Abstract

Micromorphological characteristics of seed sculpturing might be effective in circumscribing the infra-specific taxa in the genus *Vicia*. The present study was conducted to determine whether microstructural and seed coat texture data obtained from SEM images can serve as sufficient tools for delimiting *Vicia* genus. Other than visual inspections, a variety of texture-based methods, including the four conventional approaches of GLCM, LBP, LBGLCM, and SFTA, and the four pre-trained convolutional neural networks (namely, ResNet50, VGG16, VGG19, and Xception models) were employed to extract features and to classify the species of *Vicia* genus using SEM images. In a subsequent step, the four unsupervised k-means, Mean-shift, agglomerative, and Gaussian mixture classification methods were exploited to group the identified *Vicia* species based on the underlying features thus extracted. Moreover, the three supervised classifiers of multilayer perceptron network (MLP), Support Vector Machine (SVM), and k-nearest neighbor (kNN) were compared in terms of capability in discriminating the different visually-identified classes. SEM results showed that three classes might be identified based on the micromorphological character-species connections and that the differences among the species in the *Vicia* genus and the validity of *Vicia sativa* could be confirmed. Regarding the performance of the classifiers, SFTA textural descriptor outperformed the GLCM, LBP and LBGLCM algorithms but yielded a decreased accuracy compared with deep learning models. The combined Xception model and a MLP classifier was successful to discriminate the species in the *Vicia* genus with the best classification performances of 99% and 96% in training and testing, respectively.

Keywords: Scanning electron microscope (SEM), seed sculpturing, *Vicia*, micromorphology, plant taxonomy, Convolutional neural networks.

38 1. Introduction

39 Taxonomy identification methods involve destructive sampling followed by physical,
40 physiological, biochemical, and molecular determinations (Luo et al. 2021). Scanning electron
41 microscopy (SEM) and light microscopy (LM) have recently been used as important non-
42 destructive taxonomic delimitation tools for various families and genera (Ilakiya and
43 Ramamoorthy 2021; Jalal et al. 2021). SEM analysis of the seed coat surface has revealed
44 genetic diversity among *Astragaleae* and *Trifolieae* (Rashid et al. 2021), *Vicieae* (Rashid et al.
45 2018), *Geranium* (Aedo 2016), Brassicaceae (Gabr 2018), *Hypericum* (Szkudlarz and Celka
46 2016), and so on. More recently, visual assessment of SEM images has been coupled with
47 computer-aided image processing for better interpretation of SEM images to attain precise and
48 automatic identification of genera.

49 Seed surface ornamentation may be a useful and rich source of data for clustering or
50 classification based on feature determination. SEM coupled with image analysis offers a
51 powerful tool for evaluating microstructural changes (Pieniasek and Messina 2016). However,
52 the question remains whether species delimitation and identification can be solely based on
53 microstructural data and seed coat texture traits.

54 From among the few detailed studies reported on seed species identification using SEM
55 coupled with image analysis, one is Prasad *et al.* in which an image processing software was
56 used to analyze the seed coat structure of 23 cultivated and six wild sesame germplasms
57 obtained from digital and SEM images (Prasad et al. 2014). The results indicated that the seeds
58 of wild sesame species could be well differentiated from those of the cultivated varieties based
59 on shape and architectural analyses. Pieniasek and Messina conducted SEM image analysis as
60 an alternative to the analysis of the effects of freeze-drying on the microstructure and texture
61 of legume and vegetables (Pieniasek and Messina 2016). Results revealed the success of the
62 combined SEM and classical texture analysis methods as a useful tool for the investigation of
63 quality parameters.

64 Depending on the method used for extracting textural features, classical texture analysis
65 techniques can be quite diverse and varied (Ribas et al. 2020). In recent years, new methods
66 based on transfer learning with deep convolutional neural networks (CNNs) have emerged that
67 outperform the classical texture analysis in terms of the significantly better results they yield
68 (Liu X and Aldrich 2022).

69 CNNs used to classify seeds have been extensively reported on in the literature in order to
70 illustrate their applications in recognizing an individual barley kernel variety with satisfactory
71 accuracy (Kozłowski et al. 2019), determining the viability of mechanically scarified *Quercus*

72 *robur* L. seeds (Przybyło and Jabłoński 2019), identifying Chickpea (*Cicer arietinum* L.) seed
73 varieties (Taheri-Garavand et al. 2021), assessing seed germination in three different crops
74 (namely, *Zea mays*, *Secale cereale*, and *Pennisetum glaucum*) (Genze et al. 2020), and
75 obtaining high-throughput soybean seed phenotypes with efficient calculation of morphological
76 parameters (Yang et al. 2021). So far, the application of CNNs in classifying varieties based on
77 SEM images of seed coat has been mentioned in only one study, in which five different network
78 architectures were trained for classifying *Allium* seed walls based on recognizing SEM images
79 (Ariunzaya et al. 2023). Nonetheless, no study has yet been reported on the application of CNNs
80 in classifying varieties based on SEM images of seed coat surfaces.

81 It is the objective of the present work to investigate the potential of seed coat sculpturing in
82 the taxonomy of the genus *Vicia*, describe seed coat sculpturing at a specific level among the
83 Iranian species, and evaluate the diagnostic value of this character in terms of variability among
84 populations of *Vicia*. Moreover, the current study endeavors to examine the architecture of deep
85 learning convolutional neural networks and some classical texture analysis methods with
86 respect to their capabilities in categorizing *Vicia* species.

87

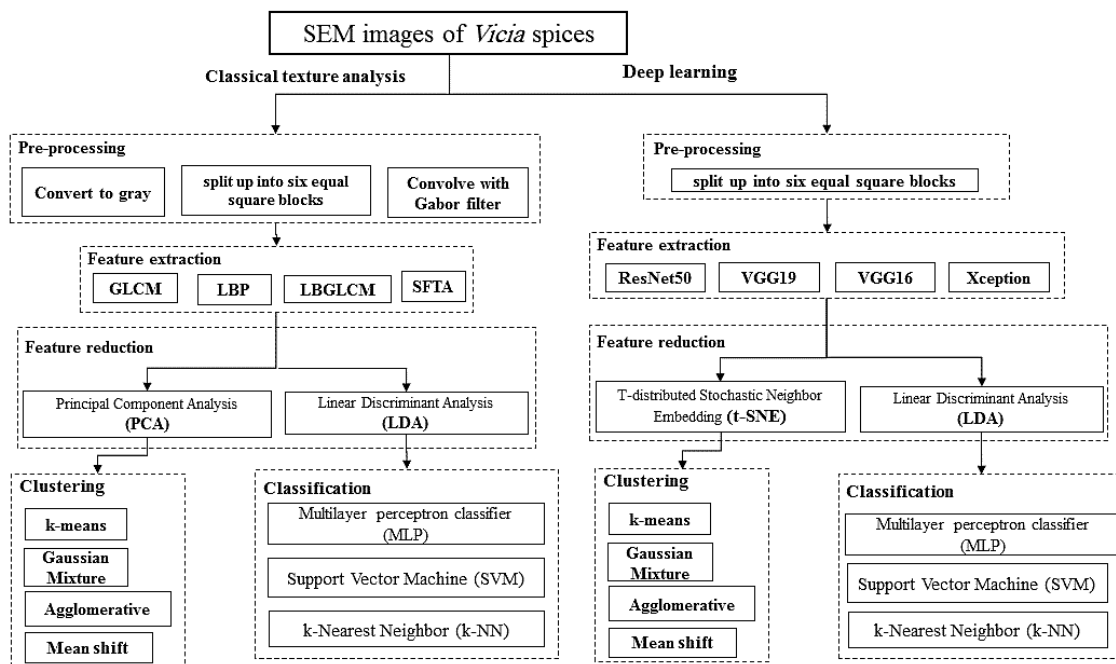
88 2. Materials and Methods

89 The methodology used in this work consists of the following five stages: 1) SEM image
90 acquisition, 2) visual observation of the SEM images thus acquired, 3) classical and deep feature
91 extraction, 4) feature dimensionality reduction, and 5) clustering and classification. The block
92 diagram illustrating the image processing and data mining steps involved in the proposed
93 methodology is presented in Figure 1.

94

95 2.1 Plant material

96 For the purposes of this study, ninety seed samples belonging to 18 *Vicia* species were
97 collected mostly from different locations in Iran. Voucher specimens of the wild specimens and
98 those obtained from the herbarium were deposited at the Herbarium Conservation Center of
99 Isfahan University of Technology (Table 1). In order to provide samples with herbarium
100 specimen labels, the accessions were grown in Chah-Anari Research Farm of Isfahan
101 University of Technology.



102
103 **Figure 1.** Block diagram of the proposed methodology.

104 **2.2 SEM image acquisition**

105 A minimum number of three mature, clean, and perfect seeds from each accession were used
 106 for taking SEM images and the subsequent analyses. The seeds were mounted on a twin-walled
 107 conductive metal stand and prepared without any dehydration using a gold grain of
 108 approximately 8-30nm thick and a BAL-TEC (Baizers) SCD 005 Sputter Coater. SEM photos
 109 from the lateral and frontal views were then taken at different magnifications (SEM, Model
 110 XL30, PHILIPS – EDAX). The density of the projections per square mm of the area at a given
 111 magnification (9 cm² at a magnification of 1000, representing 900 μm) was determined
 112 thoroughly on the display screen. Other useful specifications such as projection height, form,
 113 number, and ridge sharpness were measured and recorded. Stern (Stern 1983) terminology was
 114 used to describe the SEM images.

127 **Table 1.** Voucher specimens and herbarium data of the selected species of *Vicia* used in the
 128 SEM study of seed micromorphology.

| No. | Species/ Section | Herbarium number | Location/Province | Currently herbarium nomenclature |
|-----|---|------------------|-------------------|--|
| 1 | Sect. Anatrophyllia <i>V. koeieana</i> | 2510 | Bakhtaran | <i>V. koeieana</i> Rech. F. |
| 2 | Sect. Cracca <i>V. aucheri</i> | 5698 | Mazandaran | <i>V. aucheri</i> Boiss. |
| 3 | <i>V. cracca</i> | 99 | Isfahan | <i>Vicia cracca</i> (L.) |
| 4 | <i>V. akhmaghanica</i> | 3774 | West Azarbayegan | <i>V. akhmaghanica</i> Kazar |
| 5 | <i>V. cappadocica</i> | 19571 | West Azarbayegan | <i>V. cappadocica</i> Boiss & Bal. |
| 6 | <i>V. ciceroidea</i> | 12292 | Tehran | <i>V. ciceroidea</i> Boiss |
| 7 | <i>V. cinerea</i> | 49536 | BandarAbbas | <i>V. monantha</i> Retz. subsp. <i>monantha</i> Retz. |
| 8 | <i>V. crocea</i> | 12781 | Gorgan | <i>V. crocea</i> (Desf.) B. Fedstch. |
| 9 | <i>V. multijuga</i> | 51707 | Tehran | <i>V. multijuga</i> (Boiss.) Rech. f., V. |
| 10 | <i>V. variabilis</i> | 45924 | Fars | <i>V. variabilis</i> Grossh. |
| 11 | <i>V. villosa</i> | 26316 | Lorestan | <i>V. villosa</i> Roth |
| 12 | Sect. Ervilia <i>V. ervilia</i> | 63125 | Khozestan | <i>V. ervilia</i> (L.) Willd |
| 13 | <i>V. tetrasperma</i> | 28867 | Islamshar | <i>V. tetrasperma</i> (L.) Schreb. |
| 14 | Sect. Vicia <i>V. angustifolia</i> | 60254 | Gilan | <i>V. sativa</i> subsp. nigra (L.) Ehrh. |
| 15 | <i>V. hyrcanica</i> | 7/4 | Isfahan | <i>V. hyrcanica</i> Fisch & C. A. Mey. |
| 16 | <i>V. michauxii</i> | 20/2 | Isfahan | <i>V. michauxii</i> Spreng |
| 17 | <i>V. pregrina</i> | 24/2 | Isfahan | <i>V. pregrina</i> |
| 18 | <i>V. sativa</i> | 8714 | Mazandaran | <i>V. sativa</i> L. |

129

130 2.3 Extracting classical texture features

131 Classical image texture analysis was carried out using Open CV and Scikit-image libraries
 132 of the Python programming language. Texture features were extracted from thirty-six
 133 distinctive frontal and lateral SEM images taken at different magnifications from eighteen
 134 different *Vicia* species. Image augmentation was used to generate new transformed versions of
 135 images to increase the size and diversity of the dataset. The images were initially read and
 136 converted to grayscale before they were split up into six equal square blocks. Each block was
 137 convolved with Gabor filter, which is an orientation sensitive filter used for texture analysis to
 138 achieve the highest response at edges where texture changes (Kaus et al. 2001).

139 To extract texture features, use was made of four of the successful high-level feature extraction
 140 algorithms, including gray level co-occurrence matrix (GLCM), local binary pattern (LBP),
 141 local binary gray level co-occurrence matrix (LBGLCM), and segmentation-based fractal
 142 texture analysis (SFTA) (Table 2). These texture descriptors were computed and stored for later
 143 comparisons.

144

145

146

147

148 **Table 2** Number of features extracted by the different classical image texture analysis methods.

| Classical image texture analysis method | No. of features extracted | Variance ratio (%) | | | |
|---|---------------------------|--------------------|-------|-------|---------|
| | | PC1 | PC2 | PC3 | Overall |
| GLCM | 20 | 50.1 | 32.6 | - | 82.7 |
| LPB | 26 | 64.32 | 20.98 | - | 85.3 |
| LBGLCM | 20 | 70.15 | 19.98 | - | 90.13 |
| SFTA | 48 | 36.54 | 25.64 | 19.65 | 81.83 |

149

150 **2.4. Feature extraction using pre-trained CNN models**

151 The feasibility of CNN discrimination was investigated in the present work by loading four
 152 pre-trained models with pre-trained weights using python Tensorflow and Keras frameworks.
 153 The pre-trained convolutional networks used in this study (namely, ResNet50, VGG16,
 154 VGG19, and Xception) had been trained on features from ImageNet database and were 50, 16,
 155 19, and 71 layers deep, respectively (Table 3), with network depth defined as the largest number
 156 of sequential convolutional or fully-connected layers on a path from the input layer to the output
 157 one. The last fully-connected layer of each network was removed, the model weights were
 158 frozen, and the networks were used as feature extractors.

159 **Table 3.** Specifications of the pre-trained CNNs.

| Pretrained CNNs | Network depth | Image size | Non-trainable parameters | No. of output features | No. of PCs to reach 80% variance of the dataset |
|-----------------|---------------|------------|--------------------------|------------------------|---|
| ResNet50 | 50 | 224×224×3 | 23,587,712 | 2048 | 117 |
| VGG16 | 16 | 224×224×3 | 14,714,688 | 512 | 117 |
| VGG19 | 19 | 224×224×3 | 20,024,384 | 512 | 117 |
| Xception | 71 | 229×229×3 | 20,861,480 | 2048 | 68 |

160

161 **2.5 Dimensionality reduction**

162 The dimensionality of the feature space was reduced by Principal Component Analysis
 163 (PCA) as an unsupervised dimensionality reduction technique. The number of PCs was selected
 164 so as to reach a minimum variance of 80% of the data (Tables 2 and 3). Given the large number
 165 of principal components, the data were visualized using the t-SNE dimensionality reduction
 166 method for better performance of the deep feature extractors.

167

168 **2.5 Clustering and classification**

169 The conventional and deep feature sets were used as input to the centroid-based (i.e., k-
 170 means), density-based (i.e., mean shift), probabilistic (i.e., Gaussian mixture), and hierarchical
 171 (i.e., agglomerative) clustering methods.

172 In this study, the above clustering methods were examined with respect to their
 173 performance against three supervised similarity indices: 1) a peer-to-peer correlation metric
 174 (i.e., Jaccard coefficient), 2) an information theoretic-based approach (i.e., Normalized Mutual
 175 information (NMI)), and 3) a matching set similarity measurement index (accuracy).

176 The three supervised classifiers of multilayer perceptron (MLP), support vector machine
177 (SVM), and k-nearest neighbor (kNN) were compared in terms of their ability to recognize
178 three visually grouped species. In the back-propagation multilayer perceptron classifier, the
179 number of neurons in the input layer was set equal to the number of features chosen while that
180 of the output ones was set to 3 (equal to the three visually specified classes) with the logistic
181 sigmoid functions used in the hidden layer. The MLP was trained using the Stochastic Gradient
182 Descent (SGD) with the learning rate (η), the exponent for inverse scaling learning rate, and
183 the momentum coefficient (μ) being set to 0.001, 0.5, and 0.6, respectively. Finally, the network
184 was trained and tested for 1000 epochs. In addition, in the methodology proposed in this paper,
185 the training datasets were classified using SVM with a Gaussian Radial Basis Function (RBF)
186 kernel.

187 To develop classifiers, the dataset consisting of a total of 768 sliced blocks was randomly
188 split into training and testing (at a split ratio of 80:20) datasets. Within the training set, the 10-
189 fold cross-validation was employed to optimize the parameters and estimate the prediction
190 performance of the models.

191

192 **3. Results**

193 **3.1 Visually identified clusters**

194 Despite a generally more or less similar sculpturing pattern, the seed characters of the
195 selected *Vicia* species observed exhibited patterns of the papillose type projections (Figures 2-
196 4), representing a variety of distinct shapes, heights, and coronations. The images taken from
197 seed coat ornamentation did not show significantly adequate agreement with the classification
198 proposed in Flora Iranica (Table 3).

199 Among the samples studied, the projections were either of a primary or a secondary type
200 (only seen in *V. koeieana*). The primary ones could be described as tuberculate, colliculate, or
201 aculeate. The proximal part of the projections showed a vertical profile of acute or obtuse
202 retusus, truncate, or pungens but either curved or erect when seen from a lateral view. The tip
203 of the projections in the images taken from above appeared rounded, elliptical, or satellite
204 within the texture configuration. Based on the samples studied, three main projection type
205 groups were recognized. The first group included seed coats in which the seed surface
206 projections originated from the projection tips and continued to the background surface to form
207 Colliculate or Tuberculate projections (Figure 2 a). This group included the species *V. koeieana*,
208 *V. tetrasperma*, and *V. crocea*. Those seeds on which the projections originated from below the
209 peak to form an Aculeate were in the second group, which included the species *V. angustifolia*,

210 *V. villosa*, *V. pregrina*, *V. sativa*, *V. cappadocica*, *V. cinerea*, *V. ciceroidea*, *V. multijuga*, *V.*
211 *akhmahgancia*, *V. aucheri*, *V. cracca*, and *V. ervilia* (Figures 2b & 3). Finally, the third group
212 that contained the species *V. hyrcanica*, *V. variabilis*, and *V. michauxii* had projections starting
213 from below the peak but formed Tuberculate projections (Figure 4). Figure 5 shows some of
214 the salient seed coat topographic characters of the various species studied for use in developing
215 the key.

216 A review of the literature reveals the rival theories on how to classify species into sections.
217 For example, Boissier (Boissier and Buser 1888) divided the genus *Vicia* into two sects; namely,
218 *Sec. Euvicia* and *Sec. Cracca* (as reported in Cronquist (Cronquist 1988)) while Engler (Engler
219 1892) divided it into the four *Sec. Euvicia*, *Sec. Cracca*, *Sec. Euvicia* (link) WDKOH, and *Sec.*
220 *Euvicia* (L.) SF Grag. Other classifications have also been proposed (Fedchko 1948). No
221 satisfactory agreement was observed between the images taken from seed coat ornamentation
222 in this study and the four-way classification proposed in Flora Iranica; hence, the latter cannot
223 be reliably used as a standard reference descriptor for the classification of *Vicia* species
224 (Chrtková-Žertová 1979).

225 While most efforts on the classification of this genus have been based on such morphological
226 characters as shape, size, and hilum location (Gunn 1971; Voronchikhin 1981), analysis of more
227 species of the genus may reveal a greater variety in seed coats. This has been shown by Rashid
228 *et al.* (Rashid *et al.* 2018) in their classification of the different species of the genus *Vicia* on
229 the basis of seed characters. Extensive studies of morphological characters in other plants have
230 been almost exhaustive, leaving out only a few characters and traits. However, the great
231 differences and similarities among the plants in a species make their classification difficult.
232 Indeed, a great many species do not lend themselves to individual study to the extent that most
233 present-day scholars even claim that most observations in the past have been fallacious or
234 misinterpreted. Consequently, much emphasis is being nowadays laid on trivial traits such as
235 scale, hair, spores, or epidermal structure as descriptors for species or genus identification.

236 Pakravan *et al.* (Pakravan *et al.* 2001) showed that seed coat micro-ornamentation types are
237 especially important as identifier characters, particularly in close species that have
238 distinguishable differences such as pore-like structures on seed coat, albeit they are quite similar
239 in a general way. The authors concluded that the ornamentation types could be used as
240 distinguishing characters in very close species while judgment on more alien species had better
241 be reduced to variety level.

242 It is, therefore, impossible to draw firm conclusions on the overall *Vicia* taxonomy based on
243 the SEM analysis of only 18 species out of the 160 existing ones. Drawing upon previous work

244 on the taxonomy of *Vicia* as a model and the results obtained from the present study, it might
245 be suggested that seed coat ornamentation types (especially the size and shape of the projections
246 on the seed external coat) might be regarded as the significant and systematic characters and
247 that repeated images derived from image processing techniques might be exploited in novel
248 classifications and interpretation of the results. In addition to identification for which these
249 characters are primarily meant (e.g., recognition and pattern associations among individuals or
250 groups as additional characteristics to distinguish different *Vicia* species), these characters
251 could be utilized as the taxonomic key in plant sciences.

252

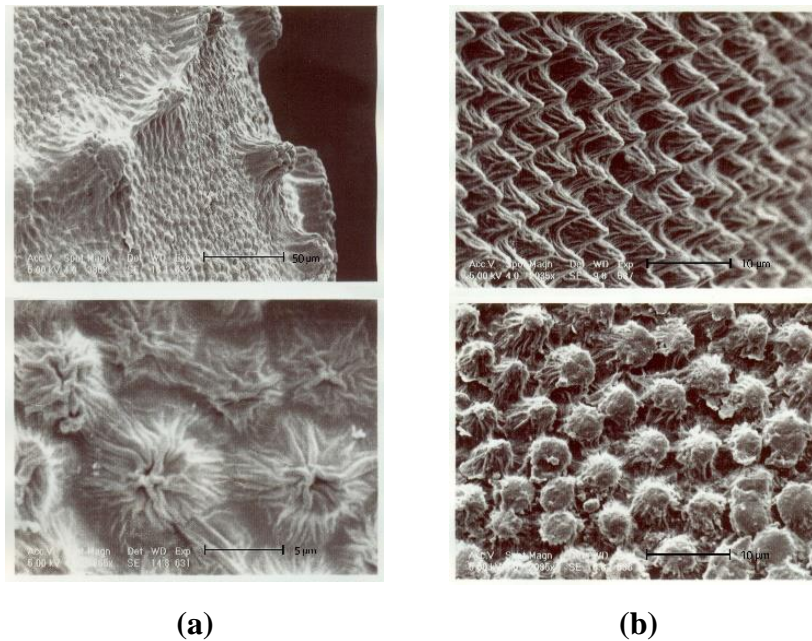
253 **3.2 Clustering performance**

254 Not all the proposed clustering approaches can generally yield satisfactory clustering results.
255 Indeed, accuracy and Jaccard indices of less than 0.55 were recorded for all the clustering
256 methods (Table 4). With all the conventional and deep feature sets, the visually classified
257 species could not be reasonably discriminated; this was evidenced by accuracy values ranging
258 from 0.36 to 0.55. While the mean-shift clustering method failed to recognize the visually
259 identified clusters so that most of the CNNs feature sets were partitioned into less than three
260 clusters, higher values of accuracy and Jaccard indices have been reported for this method. It
261 might be Jaccard and Accuracy similarity indices provide incorrect information when the
262 numbers of cluster members are dissimilar. NMI index fixes this problem by normalization.
263 The results in the present case indicated that the three k-means, agglomerative, and Gaussian
264 mixture clustering methods attained their highest NMI index values with the SFTA feature set
265 (Table 4). Moreover, when these same clustering methods were used, the silhouette coefficient,
266 which is an internal evaluation metric, was greater than 0.5 with all the feature spaces (Figure
267 6), confirming the existence of a clustering structure in the data.

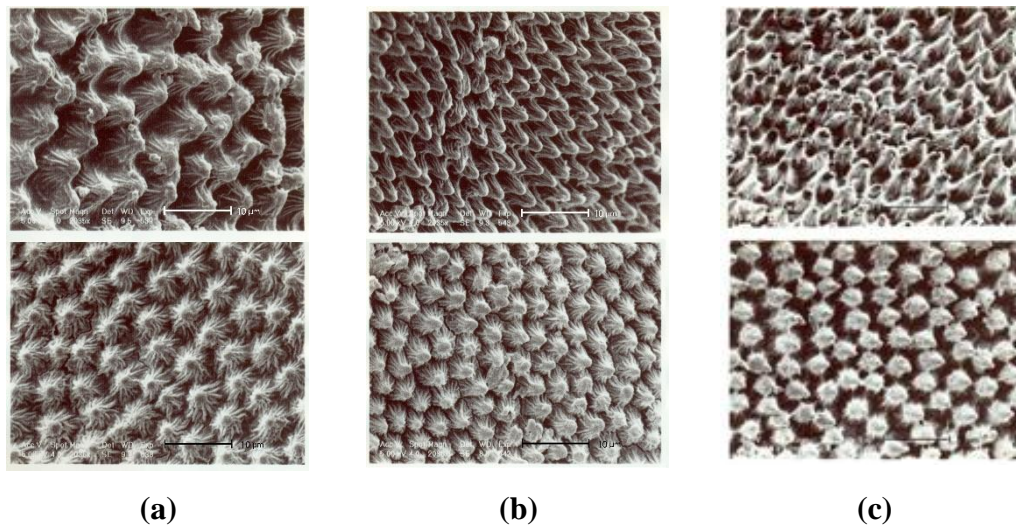
268 Chuang *et al.* (Chuang et al. 2006) mentioned that image clustering with the use of spatial
269 information such as image textural features mostly leads to undesirable results. Generally,
270 common image clustering draws upon image segmentation based on pixel colors. Moreover,
271 better clustering results can be achieved by combining color and texture features (Wei Tan et
272 al. 2018). This is while SEM images are usually described as grayscale images and are colorless
273 so that color features cannot be extracted.

274 Although the clustering based on SEM images was not successful in this study, it revealed
275 the clustering structure inherent in the data. It also showed that SEM images of the same
276 magnification and taken from a specified angle could surely improve the clustering performance
277 since image resolution, magnification, and angle of view greatly affect clustering performance.

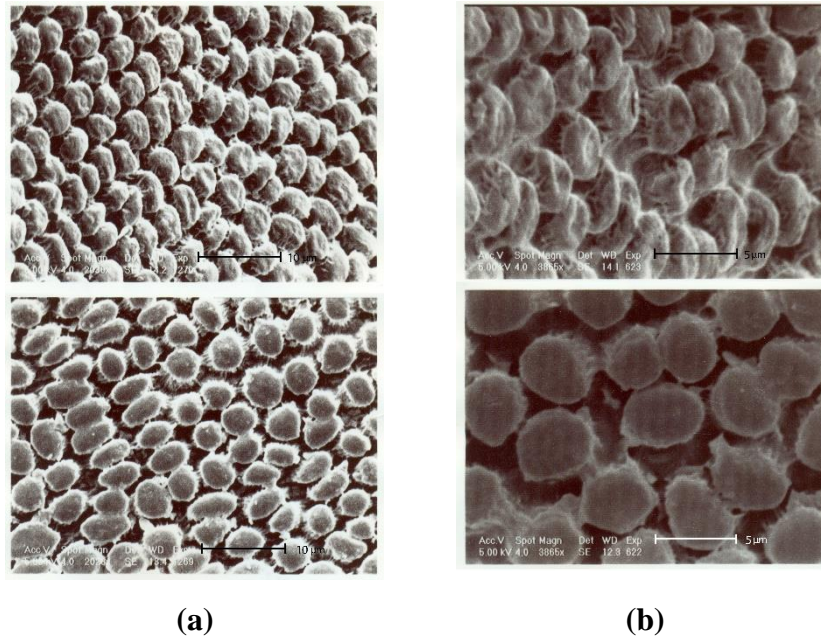
278 In conclusion, using a larger dataset with SEM images taken from a predefined direction and
 279 at known magnification ratios might be recommended if improved clustering performance and
 280 detection of the proposed method are sought.



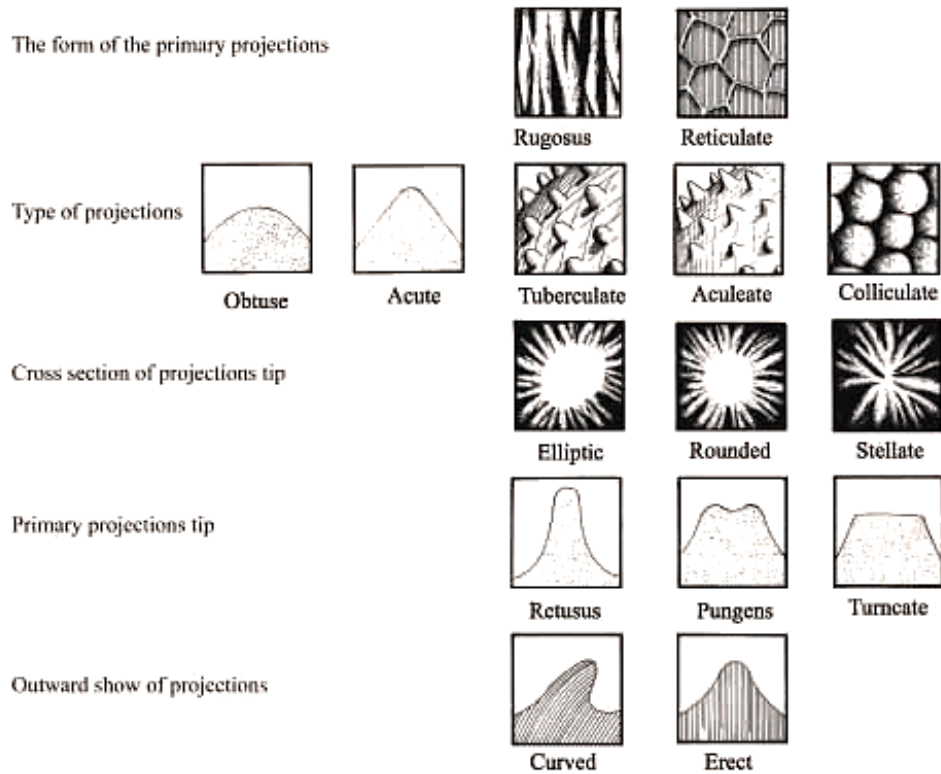
281 **Figure 2.** a) A typical primary projection in *V. koeieana* seen as a Tuberculate type of the
 282 rounded or irregular shape on the seed, b) Primary projections in *V. ervilia* seen as Colliculate
 283 projections of the short type with elliptical to irregular forms (side- and front-view images are
 284 placed in the top and bottom rows, respectively).
 285



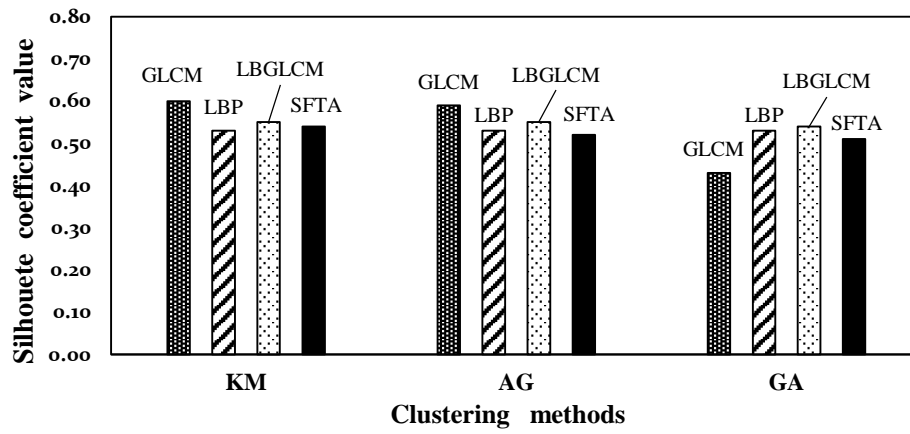
286 **Figure 3.** Primary projections in a) *V. akhmaghanica*, b) *V. craca*, and c) *V. peregrina*. The
 287 projections in all these species originate from below the peak to form an Aculeate and the
 288 proximal part of the projections exhibit a vertical profile of acute Aculeate (side- and front-
 289 view images are placed in the top and bottom rows, respectively).
 290
 291



292 **Figure 4.** Primary projections in a) *V. michauxii*, and b) *V. variabilis*. Features in the two
 293 species are seen as Tuberculate (side-view and front-view images are placed in the top and
 294 bottom rows, respectively).



295
 296 **Figure 5.** The description key for the seed coat ornamentation using Stern's terminology (Stern
 297 1983).



298

299 **Figure 6.** Computed Silhouette coefficient in evaluating the different clustering methods (KM:
 300 K-means, AG: Agglomerative, and GM: Gaussian Mixture).

301 **Table 3.** Seed micromorphological traits of eighteen *Vicia* species using SEM technology along with those of the species examined in different
 302 flora.

| Main projection type group | G1 | | | | G2 | | | | | | | | | | G3 | | | |
|---|---------------------------|-------------------------|-----------------------------|-------------------------|----|----|---|---|---|---|----|----|----|---------------------------|------------------|-------------|------------------|----|
| Flora Orientalis | | | Sect. II Cracca Series B | | | | | | | | | | | Sect. II. Cracca Series A | Sect. I. Euvicia | | Sect. I. Euvicia | |
| Flora of Turkey | Sect. Anatrophyllia Plitm | Sect. Cracca S. F. Gray | Sect. Ervum (L.) S. F. Gray | Sect. Cracca S. F. Gray | | | | | | | | | | Sect. Vicia | | Sect. Vicia | | |
| Selected <i>Vicia</i> species | 1 | 2 | 3 | 4 | 5 | 15 | 6 | 7 | 8 | 9 | 10 | 11 | 12 | 13 | 14 | 16 | 17 | 18 |
| Projection type | Ps | Pt | | Pb | | | | | | | | | | | | | | |
| Seed surface pattern | T | T | C | A | | | | | | | | | | | | T | | |
| Base and apex angles | O | | | | Q | | | | | | | | | | | | | |
| Seed shape | Er | | | | | | | | | | Cu | | | | | Er | | |
| Characteristic projections at the tip of the seed | S | | | | R | | | | | | | | | | El | | | |

303 **Legend:**

Ps: Primary and secondary projections

T: Tuberculate

O: Obtuse

Cu: abaxially curved

Pt: Primary projections at the endmost tip (peak)

A: Aculeate

Q: Acute

Er: abaxially erect

Pb: Primary projections below the peak

C: Colliculate

1. *V. koeieana* 2. *V. crocea* 3. *V. tetrasperma* 4. *V. ervilia* 5. *V. cappadocica* 6. *V. cinerea* 7. *V. cracca* 8. *V. akhmaghanica* 9. *V. aucherii*
 10. *V. multijuga* 11. *V. ciceroideae* 12. *V. sativa* 13. *V. peregrina* 14. *V. angustifolia* 15. *V. villosa* 16. *V. michauxii* 17. *V. hyrcanica* 18. *V. variabilis*

304

305

306 **Table 4.** Clustering results with classical texture and CNN selected features when both side-view
 307 and front-view images were used.

| | | ACC | JAC | NMI | | | ACC | JAC | NMI |
|--------|----|------|------|------|----------|----|-------|-------|-------|
| GLCM | KM | 0.39 | 0.24 | 0.02 | ResNet50 | KM | 0.54 | 0.37 | 0.10 |
| | AG | 0.45 | 0.29 | 0.02 | | AG | 0.42 | 0.26 | 0.10 |
| | GM | 0.38 | 0.23 | 0.02 | | GM | 0.42 | 0.26 | 0.10 |
| | MS | 0.39 | 0.24 | 0.02 | | MS | 0.5* | 0.33* | 0.00* |
| LBP | KM | 0.41 | 0.26 | 0.03 | VGG16 | KM | 0.42 | 0.26 | 0.07 |
| | AG | 0.37 | 0.23 | 0.01 | | AG | 0.50 | 0.33 | 0.05 |
| | GM | 0.39 | 0.24 | 0.02 | | GM | 0.37 | 0.25 | 0.05 |
| | MS | 0.4 | 0.25 | 0.02 | | MS | 0.5* | 0.33* | 0.00* |
| LBGLCM | KM | 0.47 | 0.31 | 0.06 | VGG19 | KM | 0.42 | 0.27 | 0.08 |
| | AG | 0.44 | 0.28 | 0.05 | | AG | 0.5 | 0.33 | 0.05 |
| | GM | 0.38 | 0.23 | 0.09 | | GM | 0.36 | 0.19 | 0.06 |
| | MS | 0.38 | 0.23 | 0.06 | | MS | 0.50* | 0.33* | 0.00* |
| SFTA | KM | 0.44 | 0.28 | 0.15 | Xception | KM | 0.33 | 0.2 | 0.07 |
| | AG | 0.50 | 0.33 | 0.16 | | AG | 0.55 | 0.37 | 0.14 |
| | GM | 0.48 | 0.32 | 0.12 | | GM | 0.40 | 0.26 | 0.09 |
| | MS | 0.47 | 0.31 | 0.08 | | MS | 0.44 | 0.29 | 0.1 |

308 KM: K-means, AG: Agglomerative, GM: Gaussian Mixture, MS: Mean-shift

309 ACC: Accuracy index, JAC: Jaccard index, NMI: Normalized Mutual Information index.

310 * Mean-shift clustering method failed to recognize the visually identified clusters, feature sets were partitioned into
 311 less than three clusters.

312

313 3.3 Classification Results

314 Based on the classification performances reported in Table 5, the best results were recorded
 315 for SFTA feature space. When both side-view and front-view images were used for the
 316 classification, a MLP with two hidden layers of 10 and 5 neurons achieved the best accuracy
 317 values of 90% and 85% in the training and testing processes, respectively. However,
 318 classification accuracy rose just when side-view images were used. In this case, a MLP with
 319 two hidden layers of 6 and 3 neurons achieved its best accuracy values of 96% and 88% in the
 320 training and testing sets, respectively. Results also revealed that the accuracy index values of
 321 SVM and kNN were not significantly different from those obtained with MLP.

322 The classification performances of different deep feature extraction models are summarized
 323 in Table 5. Clearly, three classes were better separated in the deep feature sets than they were
 324 in the conventional ones. Xception yielded the best classification result. As reported in Table
 325 5, the deep feature extraction methods outperformed the SFTA traditional textural descriptors.
 326 The features yielded by Xception and a neural network with two hidden layers of 10 and 5
 327 neurons led to better classification results with the high accuracy values of 99% and 96% in the
 328 training and testing sets, respectively. In agreement with these results, Wei Tan *et al.* (Wei Tan

329 et al. 2018) reported that the best method for the classification of plant species would be a MLP
 330 classifier with CNN features. Similar studies conducted on texture analysis of SEM images not
 331 only indicated the effectiveness of combining deep and textural features (Cai et al. 2022) but
 332 also showed that convolutional neural networks would perform equally well or better than the
 333 traditional algorithms (Liu L et al. 2016; Liu X and Aldrich 2022). The high capability of pre-
 334 trained neural networks has also been demonstrated in barley varietal classification with an
 335 accuracy value of less than 75% in varietal classification when color, texture, and
 336 morphological attributes were used and above 93% when pre-trained convolutional neural
 337 networks were employed (Kozłowski et al. 2019).

338
 339 **Table 5.** Classification results with classical texture and CNNs selected features when both
 340 side-view and front-view images were used.

| | | Accuracy index | | | | Accuracy index | |
|--------|-----|----------------|-------------|----------|-----|----------------|-------------|
| | | Train | Test | | | Train | Test |
| GLCM | MLP | 0.66 | 0.65 | ResNet50 | MLP | 0.96 | 0.74 |
| | SVM | 0.65 | 0.63 | | SVM | 0.97 | 0.73 |
| | KNN | 0.75 | 0.54 | | KNN | 0.84 | 0.71 |
| LBP | MLP | 0.74 | 0.70 | VGG16 | MLP | 0.99 | 0.75 |
| | SVM | 0.72 | 0.70 | | SVM | 0.97 | 0.72 |
| | KNN | 0.81 | 0.62 | | KNN | 0.86 | 0.70 |
| LBGLCM | MLP | 0.71 | 0.67 | VGG19 | MLP | 0.96 | 0.75 |
| | SVM | 0.71 | 0.66 | | SVM | 0.96 | 0.71 |
| | KNN | 0.81 | 0.57 | | KNN | 0.84 | 0.75 |
| SFTA | MLP | 0.90 | 0.85 | Xception | MLP | 0.99 | 0.96 |
| | SVM | 0.88 | 0.80 | | SVM | 0.99 | 0.94 |
| | KNN | 0.91 | 0.81 | | KNN | 0.98 | 0.94 |

341 MLP: Multilayer perceptron, SVM: Support Vector Machine, KNN: K-Nearest Neighbors.

342
 343 Regarding the application of pre-trained CNN models coupled with common classifiers, the
 344 results obtained proved consistent with those used VGG16+SVM in the determination of
 345 physiological disorders in apple (Buyukarikan and Ulker 2022), DenseNet169+MLP model in
 346 classifying rice plant diseases (Narmadha et al. 2022), AlexNet + SVM in assessing the severity
 347 of tomato late blight disease (Verma et al. 2020), and classifying rice plant disease (Shrivastava
 348 et al. 2019) where reached the highest accuracy of 96.11, 97.68%, 93.4% and 91.37%,
 349 respectively.

350 In conclusion, the deep models were found capable of extracting effective features for
 351 classification equally well or even better than the conventional image texture analysis methods
 352 despite the fact that they had not been trained using colorless SEM images of seed coat surfaces.

353 **4. Conclusion**

354 The paper reported on the significance of SEM image observations and analysis for the
355 classification of the different species of the genus *Vicia* into different sections. In agreement
356 with recent studies (Asadova and Asgarov 2018), the study showed that the diversity in seed
357 coat ornamentation is far less flexible and variable compared to that in growth and flowering
358 structures and that seed coat ornamentation could, thus, be exploited to disclose interspecies
359 diversity. The visual classification developed in this study showed that micromorphological
360 traits could be used as good distinctive criteria. Image analysis of *Vicia* species coupled with
361 clustering and the classification of this genus based on morphological characters
362 (microtaxonomy) could efficiently differentiate the *Vicia* species. All the pre-trained CNNs
363 deep feature extractors were found to perform equally well or better than the traditional
364 algorithms (GLCM, LBP, LBGLCM, and SFTA). Of the four CNNs used in this study,
365 Xception yielded the most reliable features and the best classification results were obtained
366 using a MLP classifier. Transfer learning was exploited to reduce the labor-intensive aspects of
367 the taxonomic classification of the genus based on seed coat surfaces. However, the scientific
368 impact of this research should be augmented by studying more samples to develop a more
369 accurate and robust classifier.

370
371 **Acknowledgment**

372 The authors would like to express their gratitude to the Deputy for Research, Isfahan
373 University of Technology, for the financial support granted.

374
375 **References**

- 376 1. Aedo, C. 2016. Taxonomic Revision of *Geranium* sect. *Polyantha* (Geraniaceae) 1. *Ann.*
377 *Missouri Bot. Gard.*, 101(4):611-635.
- 378 2. Ariunzaya, G., Kavalan, J. C. and Chung, S. 2023. Identification of seed coat sculptures
379 using deep learning. *J. Asia-Pac. Biodivers.*, 16(2):234-245.
- 380 3. Asadova, K. and Asgarov, A. 2018. Distribution and Ecobiological Research of Vetch (*Vicia*
381 L.) Species in Azerbaijan. *Int. J. Curr. Res. Biosci. Plant Biol.*, 5(7):27-36.
- 382 4. Boissier, E. and Buser, R. 1888. *Flora orientalis; sive, Enumeratio plantarum in oriente a*
383 *Graecia et Aegypto ad Indiae fines hucusque observatarum: Supplementum editore R. Buser.*
384 *apud H. Georg.*

- 385 5. Buyukarikan, B. and Ulker, E. 2022. Classification of physiological disorders in apples fruit
386 using a hybrid model based on convolutional neural network and machine learning methods.
387 *Neural Comput. Appl.* 34(19):16973-16988.
- 388 6. Cai, J., Liu, M., Zhang, Q., Shao, Z., Zhou, J., Guo, Y., Liu, J., Wang, X., Zhang, B. and Li,
389 X. 2022. Renal cancer detection: fusing deep and texture features from histopathology
390 images. *Biomed Res. Int.* 2022.
- 391 7. Chrtková-Žertová, A. 1979. *Vicia*. *Flora Iranica*. 140:16-56.
- 392 8. Chuang, K. S., Tzeng, H. L., Chen, S., Wu, J. and Chen, T. J. 2006. Fuzzy c-means clustering
393 with spatial information for image segmentation. *Comput. Med. Imaging Graph.* 30(1):9-
394 15.
- 395 9. Cronquist, A. 1988. *The evolution and classification of flowering plants*. New York
396 Botanical Garden.
- 397 10. Engler, A. 1892. *Syllabus der pflanzenfamilien*. Vol. 2. Gebrüder Borntraeger Verlag.
- 398 11. Fedchko, B. A. 1948. *Flora of the USSR (Flora SSSR)*. Vol. 13. Koeltz Scientific Books,
399 Koenigsteine.
- 400 12. Gabr, D. G. 2018. Significance of fruit and seed coat morphology in taxonomy and
401 identification for some species of Brassicaceae. *Am. J. Plant Sci.*, 9(03):380.
- 402 13. Genze, N., Bharti, R., Grieb, M., Schultheiss, S. J. and Grimm, D. G. 2020. Accurate
403 machine learning-based germination detection, prediction and quality assessment of three
404 grain crops. *Plant methods*, 16(1):1-11.
- 405 14. Gunn, C. R. 1971. *Seeds of native and naturalized vetches of North America*. US
406 Agricultural Research Service, 392.
- 407 15. Ilakiya, J. and Ramamoorthy, D. 2021. SEM and light microscopic studies in seeds of
408 *Hibiscus surattensis* L. and phylogenetic attributes in Puducherry region, India. *Geol. Ecol.*
409 *Landsc.* 5(4):269-279.
- 410 16. Jalal, M., Shaheen, S., Saddiqe, Z., Harun, N., Abbas, M. and Khan, F. 2021. Scanning
411 electron microscopic screening; Can it be a taxonomic tool for identification of traditional
412 therapeutic plants. *Microsc. Res. Tech.* 84(4):730-745.
- 413 17. Kaus, M. R., Warfield, S. K., Nabavi, A., Black, P. M., Jolesz, F. A. and Kikinis, R. 2001.
414 Automated segmentation of MR images of brain tumors. *Radiology*, 218(2):586-591.
- 415 18. Kozłowski, M., Górecki, P. and Szczypiński, P. M. 2019. Varietal classification of barley
416 by convolutional neural networks. *Biosyst. Eng.* 184:155-165.

- 417 19. Liu, L., Fieguth, P., Wang, X., Pietikainen, M. and Hu, D. 2016. Evaluation of LBP and
418 deep texture descriptors with a new robustness benchmark. *Computer Vision–ECCV: 14th*
419 *European Conference, Amsterdam, The Netherlands, October 11-14, 2016, Springer.*
- 420 20. Liu, X. and Aldrich, C. 2022. Deep learning approaches to image texture analysis in
421 material processing. *Metals*, 12(2):355.
- 422 21. Luo, T., Zhao, J., Gu, Y., Zhang, S., Qiao, X., Tian, W. and Han, Y. 2021. Classification
423 of weed seeds based on visual images and deep learning. *Inf, Process. Agric.*, 10(1): 40-51.
- 424 22. Narmadha, R., Sengottaiyan, N. and Kavitha, R. 2022. Deep transfer learning based rice
425 plant disease detection model. *Intell. Autom. Soft Comput.* 31(2): 1257-1271.
- 426 23. Pakravan, M., Hayel Moghaddam, K. and Ghahreman, A. 2001. Use of
427 micromorphological data for classification in the genus *Alcea* (Malvaceae). In *Proceeding*
428 *of deep morphology; 18-21 October; University of Vienna, Austria.*
- 429 24. Pieniasek, F. and Messina, V. 2016. Scanning electron microscopy combined with image
430 processing technique: Microstructure and texture analysis of legumes and vegetables for
431 instant meal. *Microsc. Res. Tech.*, 79(4):267-275.
- 432 25. Prasad, R., Mukherjee, K. and Gangopadhyay, G. 2014. Image-analysis based on seed
433 phenomics in sesame. *Plant Breed. Seed Sci.* 68(1):119.
- 434 26. Przybyło, J. and Jabłoński, M. 2019. Using Deep Convolutional Neural Network for oak
435 acorn viability recognition based on color images of their sections. *Comput. Electron. Agric.*
436 156:490-499.
- 437 27. Rashid, N., Zafar, M., Ahmad, M., Malik, K., Haq, I., Shah, S. N., Mateen, A. and Ahmed,
438 T. 2018. Intraspecific variation in seed morphology of tribe vicieae (Papilionoidae) using
439 scanning electron microscopy techniques. *Microsc. Res. Tech.* 81(3):298-307.
- 440 28. Rashid, N., Zafar, M., Ahmad, M., Memon, R. A., Akhter, M. S., Malik, K., Malik, N.
441 Z., Sultana, S. and Shah, S. N. 2021. Seed morphology: An addition to the taxonomy of
442 *Astragaleae* and *Trifolieae* (Leguminosae: Papilionoidae) from Pakistan. *Microsc. Res.*
443 *Tech.*, 84(5):1053-1062.
- 444 29. Ribas, L. C., Junior, J. J. dM. S, Scabini, L. F. and Bruno, O. M. 2020. Fusion of complex
445 networks and randomized neural networks for texture analysis. *Pattern Recognit.*,
446 103:107189.
- 447 30. Shrivastava, V. K., Pradhan, M. K., Minz, S. and Thakur, M. P. 2019. Rice plant disease
448 classification using transfer learning of deep convolution neural network. *Int. Arch.*
449 *Photogramm. Remote Sens. Spat. Inf. Sci.*, 42:631-635.
- 450 31. Stern, W. T. 1983. *Botanical Latin*. 3 ed. London: Thomas Nelson.

- 451 32. Szkudlarz, P. and Celka, Z. 2016. Morphological characters of the seed coat in selected
452 species of the genus *Hypericum* L. and their taxonomic value. *Biodivers. Res. Conserv.*,
453 44(1):1-9.
- 454 33. Taheri-Garavand, A., Nasiri, A., Fanourakis, D., Fatahi, S., Omid, M. and Nikoloudakis,
455 N. 2021. Automated in situ seed variety identification via deep learning: a case study in
456 chickpea. *Plants*, 10(7):1406.
- 457 34. Verma, S., Chug, A. and Singh, A. P. 2020. Application of convolutional neural networks
458 for evaluation of disease severity in tomato plant. *J. Discret. Math. Sci. Cryptogr.* 23(1):273-
459 282.
- 460 35. Voronchikhin, V. 1981. Identification of certain species of the genus *Vicia* L. from their
461 fruits and seeds.
- 462 36. Wei Tan, J., Chang, S. W., Abdul-Kareem, S., Yap, H. J. and Yong, K. T. 2018. Deep
463 learning for plant species classification using leaf vein morphometric. *IEEE/ACM Trans.*
464 *Comput. Biol. Bioinform.*, 17(1):82-90.
- 465 37. Yang, S., Zheng, L., He, P., Wu, T., Sun, S. and Wang, M. 2021. High-throughput
466 soybean seeds phenotyping with convolutional neural networks and transfer learning. *Plant*
467 *Methods*, 17(1):50.

468
469
470
471
472
473
474
475
476
477
478
479
480
481
482
483
484
485
486
487
488
489

490 طبقه بندی برخی از گونه های *Vicia* ایرانی با استفاده از تحلیل و تفسیر بافت تصاویر SEM به روش مرسوم
491 و یادگیری عمیق

492 مهرنوش جعفری، سید علی محمد میرمحمدی میبدی، و محمد حسین اهتمام

493 **چکیده**

494 ویژگی های میکرومورفولوژیکی برجستگی های روی سطح دانه ممکن است در شناسایی گونه های جنس *Vicia* مؤثر باشند. مطالعه
495 حاضر به منظور تعیین اینکه آیا داده های ریزساختاری و تزئینات پوشش دانه به دست آمده از تصاویر SEM می توانند به عنوان ابزار
496 کافی برای شناسایی جنس *Vicia* استفاده شوند، انجام شد. به غیر از بررسی بصری، انواع روش های مبتنی بر بافت، از جمله چهار
497 روش مرسوم GLCM، LBP، LBGLCM، و SFTA، و چهار شبکه عصبی کانولوشن از پیش آموزش دیده (یعنی ResNet50،
498 VGG16، VGG19، و Xception) برای استخراج ویژگی ها و دسته بندی گونه های جنس *Vicia* با استفاده از تصاویر SEM
499 استفاده شد. در مرحله بعدی، چهار روش طبقه بندی Gaussian mixture و agglomerative، Meanshift، k-means
500 بدون نظارت برای گروه بندی گونه های *Vicia* شناسایی شده بر اساس ویژگی های استخراج شده، مورد بهره برداری قرار گرفتند.
501 همچنین، سه طبقه بندی کننده با نظارت شامل شبکه پرسپترون چندلایه (MLP)، ماشین بردار پشتیبان (SVM) و k-نزدیک ترین
502 همسایه (kNN) از نظر قابلیت در تمایز دسته های مختلف شناسایی شده به روش بصری، مقایسه شدند. نتایج SEM نشان داد که
503 ممکن است سه کلاس بر اساس پیوندهای ریزمورفولوژیکی صفت-گونه شناسایی شود و تفاوت بین گونه ها در جنس *Vicia* و
504 اعتبار *Vicia sativa* قابل تأیید است. با توجه به نتایج طبقه بندی کننده ها، عملکرد توصیفگر بافتی SFTA از الگوریتم های GLCM،
505 LBP و LBGLCM بهتر بود اما عملکرد ضعیف تری نسبت به مدل های یادگیری عمیق، نشان داد. مدل ترکیبی Xception و
506 MLP در تفکیک گونه ها در جنس *Vicia* با بهترین عملکرد طبقه بندی به ترتیب 99٪ و 96٪ در آموزش و آزمون موفق بود.
507